Journal of Integrative Neuroscience

J. Integr. Neurosci. **2026**; 25(4): 49070
https://doi.org/10.31083/JIN49070

Original Research

Regional Associations Between Ocular Vascular Parameters and Enlarged Perivascular Spaces in the Basal Ganglia and Centrum Semiovale

Nuo Ma[1,†], Juan Tao[2,†], Qiong Dong[1,†], Qiuyue Yu[3], Haichao Wang[1], Ping Li[2], Quan Yuan[2], Aiping Jin[3,*], Peng Gao[2,*], Li Gong[3,*]

[1]Department of Neurology, Shanghai Tenth People's Hospital, School of Medicine, Tongji University, 200092 Shanghai, China
[2]Department of Ophthalmology, Shanghai Tenth People's Hospital, School of Medicine, Tongji University, 200092 Shanghai, China
[3]Department of Neurology, Tongren Hospital, School of Medicine, Shanghai JiaoTong University, 200336 Shanghai, China
*Correspondence: 13402140058@163.com (Aiping Jin); neocloudy@hotmail.com (Peng Gao); gongli@tongji.edu.cn (Li Gong)
[†]These authors contributed equally.

Academic Editor: Bettina Platt
Submitted: 4 August 2025 Revised: 13 January 2026 Accepted: 26 January 2026 Published: 22 April 2026

Abstract

Background: Enlarged perivascular spaces (EPVS) represent a hallmark imaging feature of cerebral small vessel disease. The ocular vasculature is an anatomical extension of cerebral vessels, constituting part of the microvascular system; however, the relationship between ocular vascular characteristics and EPVS remains poorly understood. In this study, we examined the association between ocular vascular parameters and the regional distribution of EPVS in patients with minor stroke. **Methods**: Patients diagnosed with minor stroke between 2021 and 2024 were prospectively enrolled. Ocular vascular characteristics were assessed using optical coherence tomography angiography (OCTA) and ophthalmic arterial ultrasound (OAU), while 3.0 T magnetic resonance imaging (MRI) was performed to evaluate EPVS in the centrum semiovale (CSO) and basal ganglia (BG). Demographic characteristics, clinical risk factors, neuroimaging findings, and laboratory data were recorded at admission. **Results**: A total of 111 participants were enrolled, with a mean age of 65.23 $\pm$ 7.62 years; 43.24% were female. At baseline, 43 patients (38.74%) had high CSO-EPVS burden, and 61 (54.95%) had high BG-EPVS burden. In multivariate regression analysis, superficial retinal capillary plexus perifoveal density (odds ratio [OR] = 0.87, $p = 0.020$) measured by OCTA and diabetes mellitus were independently associated with BG-EPVS, whereas the resistive index of the ophthalmic artery (OR = 1.33, $p < 0.001$) measured by OAU was independently and positively associated with CSO-EPVS. **Conclusions**: Ocular microvascular density was associated with BG-EPVS, whereas ocular vascular elasticity was associated with CSO-EPVS. These findings support the hypothesis that these EPVS subtypes arise from distinct vascular mechanisms – microvascular hypoperfusion versus reduced vascular elasticity.

Keywords: enlarged perivascular spaces; optical coherence tomography angiography; ophthalmic artery; ultrasonography; doppler; microvascular dysfunction

1. Introduction

Perivascular spaces (PVS) are fluid-filled compartments that surround penetrating arteries, capillaries, veins, and venules as they extend from the brain surface into the parenchyma. When these spaces become dilated, they are termed enlarged perivascular spaces (EPVS) [1]. EPVS are predominantly located in the basal ganglia (BG) and centrum semiovale (CSO), regions thought to predominantly represent hypertensive microangiopathy and cerebral amyloid angiopathy (CAA), respectively [2]. Age, hypertension, gender, and white matter lesions are more strongly associated with BG-EPVS, whereas arteriosclerosis, smoking, and deep microbleeds are more strongly associated with CSO-EPVS [3–5], suggesting distinct underlying pathophysiological mechanisms. EPVS typically progress slowly and continuously, making their temporal dynamics challenging to investigate in the general population [6]. Patients with minor stroke may represent an early or relatively mild stage of cerebral small vessel disease (CSVD), with fewer confounding factors such as large-vessel occlusion, cerebral edema, or extensive tissue damage, and are more amenable to recruitment and follow-up. Accordingly, several studies on cerebral small vessel disease have focused on this population [3,7,8].

The retina and brain share anatomical, physiological, and embryological similarities in cell types, vasculature, and immune responses [9]. Because the retinal microvasculature shares structural and functional similarities with the cerebral vascular system, alterations in retinal microvascular parameters may provide valuable insights into cerebrovascular and neurodegenerative disorders [10]. Consequently, optical coherence tomography angiography (OCTA) and ophthalmic arterial ultrasound (OAU) may offer a unique perspective on brain function and a range of neurological disorders [11]. Previous study has focused on associations between ocular vascular alterations and

Alzheimer's disease (AD), multiple sclerosis (MS), or various optic neuropathies (ON) [12]. However, evidence regarding the relationship between ocular vascular characteristics and EPVS among patients with minor stroke remains limited. A recent study has investigated the association between retinal vascular alterations and EPVS, indicating that greater severity of retinal arteriosclerosis is linked to increased EPVS burden [13]. Notably, one study found inverse correlations between EPVS grade and number and both the central retinal arteriolar equivalent (CRAE) and the arteriole-to-venule ratio (AVR); however, the precise anatomical locations of the EPVS were not specified [14].

Based on the foregoing considerations, this study aimed to further explore the association between EPVS burden in different brain regions and ocular vascular characteristics in patients with minor stroke.

2. Methods

2.1 Participants

A prospective observational study was conducted, enrolling all consecutive patients admitted to Shanghai Tenth People's Hospital, Tongji University, between 1 January 2021 and 1 January 2024 who met the inclusion criteria for minor stroke. The inclusion criteria were as follows: patients diagnosed with ischemic stroke based on computed tomography (CT) or magnetic resonance imaging (MRI), following the 2013 American Heart Association/American Stroke Association guidelines; stroke onset within 7 days; age over 18 years; National Institutes of Health Stroke Scale (NIHSS) score $\leq$3; and no history of prior cognitive impairment. Each participant underwent a comprehensive ophthalmic evaluation—including OCTA and OAU—and a detailed brain MRI examination. Participants were excluded if they had a history of retinal or choroidal diseases (including age-related macular degeneration, retinal vein occlusion, uveitis, retinal detachment, or central serous chorioretinopathy), glaucoma or other optic neuropathies, a history of intraocular surgery, acute large-territory cerebral infarction or cerebral hemorrhage, or brain tumors. Assessment at inclusion encompassed clinical and demographic information, including age, gender, body mass index (BMI), hypertension (history or sustained blood pressure $>$140/90 mmHg), diabetes mellitus (history or fasting blood glucose $\geq$7.0 mmol/L or HbA1c $\geq$6.5%), smoking status, and history of recurrent stroke.

2.2 Assessment of Enlarged Perivascular Spaces (EPVS)

Brain MRI was performed using a 3.0-T scanner (Magnetom Verio 3.0 T, Siemens Medical Solutions, Germany) with high-end gradients of 30 mT/m. The imaging protocol consisted of T1-weighted imaging (T1WI: TR = 140 ms, TE = 2.46 ms, FOV = 38 cm, slice thickness = 6 mm, interslice interval = 1.5 mm, matrix = 320 $\times$ 180) and T2-weighted imaging (T2WI: TR = 1300 ms, TE = 92 ms, FOV = 38 cm, slice thickness = 5 mm, interslice interval = 1 mm, matrix = 380 $\times$ 268), along with fluid-attenuated inversion recovery (FLAIR) and diffusion-weighted imaging (DWI) sequences. All images were assessed on a radiological workstation by two independent raters—a senior neuroradiologist and a neurology PhD student—both blinded to participants' baseline demographic and clinical information.

EPVS were defined as round or linear cerebrospinal fluid–isointense lesions smaller than 3 mm (hyperintense on T2 and hypointense on T1/FLAIR) following the path of penetrating arteries. After reviewing all relevant slices, the maximum number of EPVS observed on one side of the brain was recorded. EPVS burden in the CSO and BG was visually rated and classified as high or low. Consistent with prior studies [15,16], a threshold of $\geq$20 EPVS was used to define high burden. Inter-rater reliability was evaluated using a two-way random-effects intraclass correlation coefficient (ICC), demonstrating good agreement between raters (ICC = 0.82, 95% CI: 0.71–0.88). Any discrepancies were resolved by consensus to establish the final EPVS burden. Periventricular and deep white matter lesions were evaluated according to the Fazekas scale, with consensus reached between the raters. MRI scans with severe motion artifacts or insufficient contrast that precluded reliable assessment were excluded, whereas images with minor artifacts that did not affect EPVS visualization were retained.

2.3 Optical Coherence Tomography Angiography (OCTA)

The retinal microvasculature was evaluated using an RTVue XR Avanti spectral-domain OCT system (Optovue, Inc., Fremont, CA, USA) with integrated AngioVue software (RTVue-XR version 2017.1.0.155, Optovue, Inc.) for quantitative analysis. OCTA was used to scan the central retinal region (6 $\times$ 6 mm) and the peripapillary area of the optic disc (4.5 $\times$ 4.5 mm). Images with insufficient signal quality [signal strength index (SSI) $<$50] or high motion artifact scores ($>$3) were excluded. Scans were acquired from both eyes under low-lighting conditions using a spectral-domain OCT with an angiography module. All images of the foveal avascular zone (FAZ), superficial retinal capillary plexus (SRCP), and deep retinal capillary plexus (DRCP) in the macular region were analyzed to automatically calculate vessel density (VD). The SRCP was segmented from the internal limiting membrane (ILM) to 10 µm above the inner plexiform layer (IPL), while the DRCP was segmented from 10 µm above the IPL to 10 µm below the outer plexiform layer (OPL). Two concentric macular zones in the SRCP and DRCP were analyzed, comprising a parafoveal inner zone (0.3–1.5 mm from the fovea) and a perifoveal outer zone (1.5–3.0 mm from the fovea). The thickness of the retinal nerve fiber layer (RNFL) in the superficial and deep retina was also measured. Additionally, the peripapillary capillary density, inside disc density, and peripapillary RNFL of the optic disc were measured automatically.

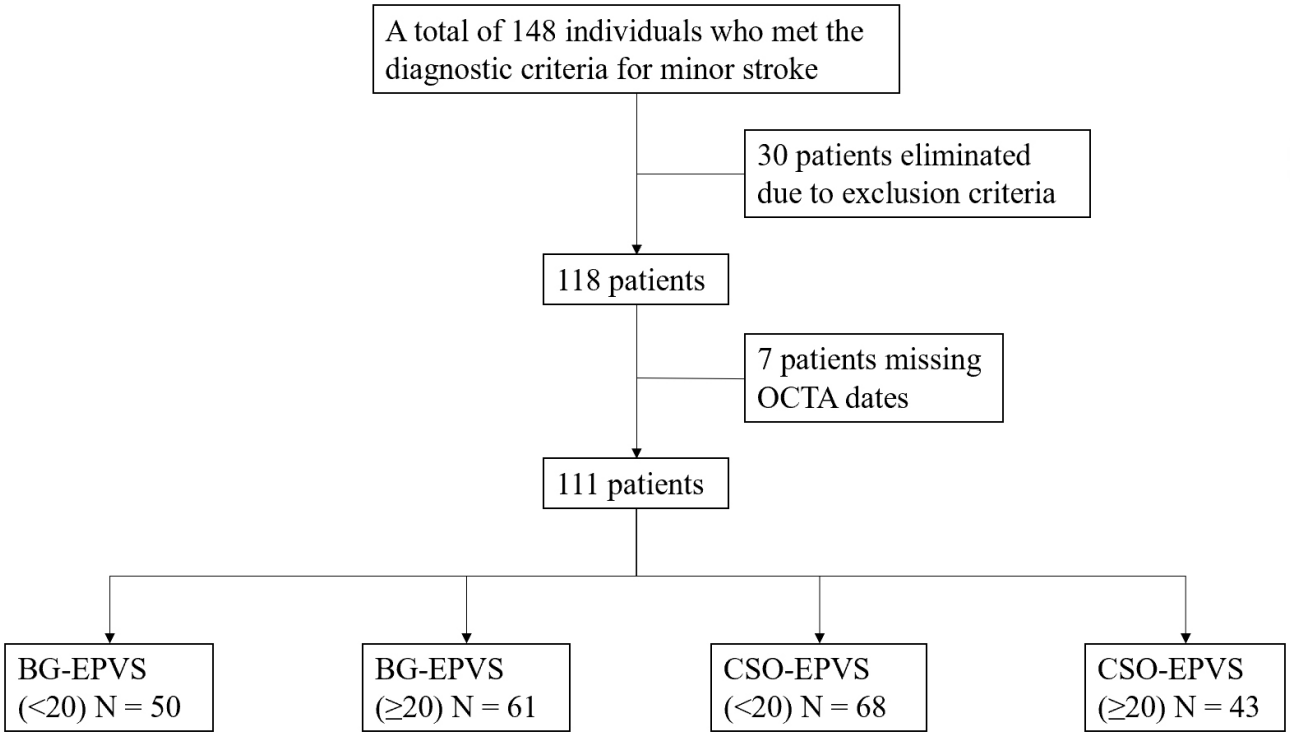

Fig. 1. Study flow chart. BG, Basal ganglia; EPVS, enlarged perivascular spaces; CSO, centrum semiovale; OCTA, optical coherence tomography angiography.

2.4 Ophthalmic Arterial Ultrasound (OAU)

A 7.5-MHz linear transducer (PLT-704SBT, Canon Medical Systems Corporation, Ōta, Tokyo, Japan) was gently applied transversely to the patient's closed upper eyelid with conduction gel by a sonographer. Pulsed-wave Doppler (Canon Medical Systems Corporation, Ōta, Tokyo, Japan) was then used to record three to five similar waveforms, with the insonation angle maintained below 20°, a 2-mm sample gate, depth of 3.0–4.5 cm, high-pass filter at 50 Hz, and pulse repetition frequency set at 125 kHz. Color Doppler ultrasonography (Canon Medical Systems Corporation) was used to identify the ophthalmic artery (OA), central retinal artery (CRA), posterior ciliary artery (PCA), and central retinal vein (CRV), and to evaluate the peak systolic velocity (PSV), end-diastolic velocity (EDV), and resistive index (RI) of each artery.

2.5 Data Analysis

Data were analyzed using SPSS 27.0 for Windows (IBM Corp., Armonk, NY, USA), with $p < 0.05$ considered statistically significant. Mean values of both eyes were used when available; if one eye was excluded, the value from the remaining eye was used. The Shapiro–Wilk test was used to assess normality. Normally distributed continuous variables were summarized as mean ± SD (standard deviation), while non-normally distributed variables were reported as median (interquartile range, IQR) and analyzed using the *t*-test or Wilcoxon rank-sum test, respectively. Categorical variables were expressed as counts (percentages) and compared using Fisher's exact test or Pearson's chi-square test. Univariable and multivariable logistic regression analyses were performed to identify risk factors for high compared with low EPVS burden in the BG and CSO, with high burden defined as ≥20 EPVS per region. To avoid multicollinearity, correlations between candidate variables were evaluated using pairwise correlation coefficients and variance inflation factors (VIFs).

3. Results

3.1 Baseline Characteristics of Study Participants

Overall, 148 participants meeting the diagnostic criteria for minor stroke were enrolled in the study; 30 were eliminated due to exclusion criteria and 7 patients had missing OCTA data. Ultimately, 111 individuals (43.24% female) were included in the final analysis (Fig. 1), with a mean age of 65.23 ± 7.62 years. The demographic features and other characteristics of the patients are provided in Table 1. Among the patients, 45.95% had diabetes mellitus, 33.33% had a history of smoking, 36.04% had recurrent stroke, and more than half (65.77%) had hypertension. Overall, 43 patients (38.74%) had high CSO-EPVS burden, and 61 (54.95%) had high BG-EPVS burden. Low EPVS burden was observed more frequently in female patients (56.00% vs. 32.79%; $p = 0.014$ for BG-EPVS; 51.47% vs. 30.23%; $p = 0.028$ for CSO-EPVS). High BG-EPVS burden was observed more frequently among patients with dia-

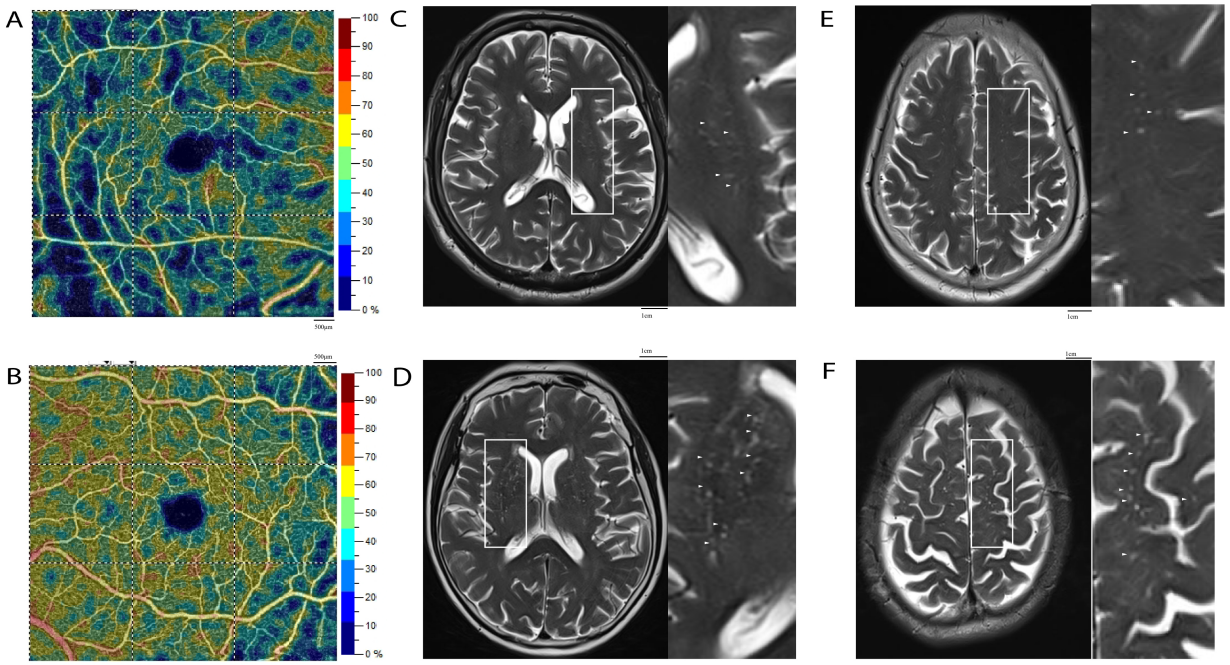

Fig. 2. Different densities of superficial retinal capillary plexus (SRCP) and different burdens of EPVS. (A) Low SRCP density on OCTA. (B) High SRCP density on OCTA. (C) Low BG-EPVS burden. (D) High BG-EPVS burden. (E) Low CSO-EPVS burden. (F) High CSO-EPVS burden. Scale bars: 500 µm and 1cm in OCTA images (A,B); 1 cm in MRI images (C–F). Annotations: White solid boxes indicate the region of interest (ROI) for a magnified view; small white arrows point to representative EPVS.

Table 1. Baseline characteristics in patients with high versus low EPVS burden in the CSO and BG.

Characteristic	BG-EPVS (<20)	BG-EPVS (≥20)	*p* value	CSO-EPVS (<20)	CSO-EPVS (≥20)	*p* value
	N = 50	N = 61		N = 68	N = 43	
Age, mean ± SD	63.50 ± 8.19	66.59 ± 6.92	0.054	64.83 ± 6.83	65.94 ± 8.91	0.506
Gender (female) (%)	28 (56.00)	20 (32.79)	0.014*	35 (51.47)	13 (30.23)	0.028*
Diabetes mellitus (%)	16 (32.00)	35 (57.38)	0.008*	29 (42.65)	22 (51.16)	0.380
Hypertension (%)	33 (66.00)	40 (65.57)	0.962	46 (67.65)	27 (62.79)	0.599
History of smoke (%)	13 (26.00)	24 (39.34)	0.138	21 (30.88)	16 (37.21)	0.491
Recurrent stroke (%)	17 (34.00)	23 (37.70)	0.686	25 (36.76)	15 (34.88)	0.841
Fazekas pWML score, mean ± SD	1.33 ± 0.57	1.49 ± 0.73	0.244	1.29 ± 0.62	1.64 ± 0.70	0.018*
Fazekas dWML score, mean ± SD	0.98 ± 0.92	1.27 ± 0.90	0.121	1.03 ± 0.96	1.33 ± 0.82	0.134
BMI, mean ± SD	24.09 ± 2.66	24.14 ± 2.78	0.935	24.03 ± 2.76	24.27 ± 2.67	0.628

Abbreviations: pWML, periventricular white matter lesion; dWML, deep white matter lesion; BMI, body mass index; SD, standard deviation.

*Statistically significant difference ($p < 0.05$).

betes mellitus, whereas high CSO-EPVS burden was significantly associated with Fazekas score (1.29 ± 0.62 vs. 1.64 ± 0.70; $p = 0.018$) in periventricular white matter lesions (pWML). Fig. 2 illustrates the burden of EPVS in different regions and varying retinal vascular densities.

3.2 Comparison of Ophthalmic Parameters by Regional EPVS Burden

A comparison of OCTA examination characteristics between patients with high and low EPVS burden in the CSO and BG is shown in Table 2. Patients with high BG-EPVS or CSO-EPVS burden were more likely to have lower retinal microvasculature density in the macular region, including SRCP parafoveal density, SRCP perifoveal density, DRCP parafoveal density, and DRCP perifoveal density. Furthermore, high BG-EPVS burden was significantly associated with low inside disc density (50.43% vs. 47.58%; $p = 0.015$) in the optic disc, whereas no significant difference was found between groups in CSO-EPVS burden (49.70% vs. 47.95%; $p = 0.059$). The superficial, deep, and peripapillary RNFL thickness and FAZ did not differ significantly between subjects with high EPVS burden and those with low EPVS burden. As shown in Table 3, ophthalmic arterial ultrasound was performed to determine the RI, PSV,

Table 2. OCTA characteristics in patients with high versus low EPVS burden in the CSO and BG.

Characteristic	BG-EPVS (<20) N = 50	BG-EPVS (≥20) N = 61	*p* value	CSO-EPVS (<20) N = 68	CSO-EPVS (≥20) N = 43	*p* value
SRCP ParaFovea density (%)	52.25 (50.47, 54.64)	46.65 (39.24, 49.92)	<0.001*	51.10 (48.68, 54.17)	46.65 (38.70, 49.92)	<0.001*
SRCP PeriFovea density (%)	50.47 (48.50, 51.77)	46.10 (41.29, 49.14)	<0.001*	49.95 (46.81, 51.91)	46.10 (41.29, 49.14)	<0.001*
DRCP ParaFovea density (%)	53.42 (51.30, 56.19)	50.10 (43.88, 54.26)	<0.001*	52.73 (48.60, 56.08)	50.18 (44.64, 53.48)	0.044*
DRCP PeriFovea density (%)	49.20 (44.26, 52.51)	46.07 (37.04, 49.44)	0.001*	48.34 (43.09, 52.42)	45.72 (38.74, 48.78)	0.014*
FAZ Area (mm^2)	0.33 (0.27, 0.43)	0.30 (0.22, 0.44)	0.576	0.32 (0.23, 0.42)	0.35 (0.24, 0.45)	0.552
sRNFL (μm)	102.85 (96.43, 107.93)	100.90 (87.40, 106.10)	0.321	102.60 (95.10, 107.58)	100.30 (85.25, 104.70)	0.205
dRNFL (μm)	192.15 (186.80, 198.88)	192.70 (177.60, 204.70)	0.870	192.25 (185.25, 200.28)	193.70 (178.25, 205.10)	0.773
pRNFL (μm)	107.72 (98.97, 119.95)	108.56 (99.89, 121.40)	0.770	107.72 (97.83, 120.18)	112.03 (103.99, 121.22)	0.283
Inside disc density (%)	50.43 (47.49, 53.37)	47.58 (44.61, 50.73)	0.015*	49.70 (45.60, 53.66)	47.95 (43.53, 50.82)	0.059
Peripapillary capillary density (%)	51.63 (49.67, 53.21)	51.04 (45.66, 53.66)	0.672	50.98 (47.50, 53.52)	52.27 (48.68, 53.64)	0.445

Abbreviations: DRCP, deep retinal capillary plexus; FAZ, foveal avascular zone; sRNFL, superficial retinal nerve fiber layer; dRNFL, deep retinal nerve fiber layer; pRNFL, peripapillary retinal nerve fiber layer.

*Statistically significant difference ($p < 0.05$).

Table 3. OAU characteristics in patients with high versus low EPVS burden in the CSO and BG.

Characteristic	BG-EPVS (<20) N = 50	BG-EPVS (≥20) N = 61	*p* value	CSO-EPVS (<20) N = 68	CSO-EPVS (≥20) N = 43	*p* value
OA						
RI, mean ± SD	73.65 ± 5.05	73.12 ± 4.88	0.617	72.42 ± 4.88	74.92 ± 4.69	0.024*
PSV (cm/s)	43.25 (37.63, 48.88)	38.00 (31.00, 47.75)	0.090	42.00 (35.00, 55.00)	40.00 (29.00, 49.00)	0.176
EDV (cm/s)	10.75 (9.50, 13.00)	10.25 (7.63, 12.50)	0.375	11.00 (9.00, 15.00)	10.00 (7.00, 11.00)	0.056
CRA						
RI, mean ± SD	61.75 ± 7.10	61.10 ± 7.34	0.687	61.96 ± 7.99	60.39 ± 5.64	0.337
PSV (cm/s)	16.50 (15.00, 20.50)	16.50 (12.63, 21.00)	0.363	16.00 (14.00, 20.00)	18.00 (13.00, 23.00)	0.996
EDV (cm/s)	10.50 (9.00, 13.75)	10.00 (7.00, 15.00)	0.374	7.00 (5.00, 8.00)	7.00 (5.00, 9.00)	0.625
PCA						
RI, mean ± SD	61.61 ± 6.40	60.21 ± 5.52	0.285	60.75 ± 5.80	60.90 ± 6.22	0.914
PSV (cm/s)	20.00 (16.50, 22.75)	18.25 (14.13, 23.38)	0.222	20.00 (15.00, 24.00)	19.00 (14.00, 21.00)	0.867
EDV (cm/s)	7.50 (6.50, 9.00)	7.25 (5.00, 9.00)	0.497	8.00 (6.00, 10.00)	7.00 (5.00, 9.00)	0.477
CRV	8.50 (7.00, 9.50)	7.50 (6.00, 9.50)	0.288	8.00 (6.00, 9.00)	8.00 (6.00, 9.00)	0.221

Abbreviations: OAU, ophthalmic arterial ultrasound; OA, ophthalmic artery; CRA, central retinal artery; PCA, posterior ciliary artery; CRV, central retinal vein; RI, resistive index; PSV, peak systolic velocity; EDV, end-diastolic velocity.

*Statistically significant difference ($p < 0.05$).

and EDV of three arteries and one vein. High CSO-EPVS burden was more frequent in patients with high RI of the OA (72.42 ± 4.88 vs. 74.92 ± 4.69; $p = 0.024$), while no difference was observed between high and low BG-EPVS burden groups. High EPVS burden was also more frequently observed in patients with low blood flow velocity, although no significant differences in PSV or EDV of the OA were found. RI, PSV, and EDV of the CRA and PCA were not associated with EPVS burden, nor was the blood flow velocity of the CRV.

3.3 Risk Factors for Regional EPVS Burden

In the univariate logistic regression analysis (Table 4), BG-EPVS and CSO-EPVS burden were negatively correlated with SRCP parafoveal density, SRCP perifoveal density, DRCP parafoveal density, DRCP perifoveal density, and inside disc density in patients with minor stroke. A significant correlation was found between BG-EPVS burden and gender (odds ratio [OR] = 0.38, $p = 0.015$), as well as with diabetes mellitus (OR = 2.86, $p = 0.008$). The analysis also demonstrated stronger associations between high CSO-EPVS burden and gender (OR = 0.41, $p = 0.030$), high

Table 4. Univariate logistic regression analysis for EPVS in different regions.

Characteristic	BG-EPVS			CSO-EPVS		
	OR	95% CI	*p* value	OR	95% CI	*p* value
Demographic statistics						
Age	1.06	0.99–1.12	0.061	1.02	0.96–1.08	0.502
Gender (female)	0.38	0.18–0.83	0.015*	0.41	0.18–0.92	0.030*
Diabetes mellitus	2.86	1.31–4.25	0.008*	1.41	0.65–3.03	0.381
Hypertension	1.02	0.46–2.24	0.962	0.81	0.37–1.80	0.600
Smoking	1.85	0.82–4.17	0.140	1.33	0.59–2.97	0.491
Recurrent stroke	1.18	0.54–2.57	0.686	0.92	0.42–2.05	0.841
Fazekas pWML score	1.47	0.77–2.81	0.243	2.79	1.14–4.27	0.022*
Fazekas dWML score	1.45	0.90–2.34	0.123	1.44	0.89–2.31	0.121
BMI	1.01	0.86–1.17	0.934	1.03	0.88–1.21	0.678
OCTA						
SRCP ParaFovea density	0.79	0.70–0.89	<0.001*	0.90	0.84–0.96	0.001*
SRCP PeriFovea density	0.83	0.75–0.93	<0.001*	0.87	0.80–0.95	0.002*
DRCP ParaFovea density	0.89	0.82–0.96	0.003*	0.95	0.90–0.99	0.024*
DRCP PeriFovea density	0.90	0.84–0.96	0.002*	0.93	0.88–0.99	0.016*
FAZ Area	2.03	0.58–3.13	0.272	1.66	0.72–3.85	0.234
sRNFL	0.99	0.97–1.02	0.581	0.99	0.96–1.01	0.250
dRNFL	0.99	0.97–1.02	0.661	0.99	0.97–1.02	0.775
pRNFL	1.01	0.98–1.03	0.574	1.02	0.99–1.05	0.187
Inside disc density	0.93	0.86–0.99	0.041*	0.92	0.85–0.99	0.029*
Peripapillary capillary density	0.98	0.93–1.04	0.531	1.03	0.96–1.09	0.448
Ophthalmic artery ultrasound						
OA						
RI, mean ± SD	1.00	0.92–1.09	0.949	1.16	1.05–1.28	0.005*
PSV	0.99	0.96–1.02	0.464	0.97	0.94–1.01	0.123
EDV	0.99	0.88–1.11	0.847	0.93	0.82–1.06	0.288
CRA						
RI, mean ± SD	0.99	0.93–1.05	0.683	0.97	0.91–1.00	0.334
PSV	0.95	0.89–1.03	0.204	0.99	0.91–1.09	0.972
EDV	0.88	0.70–1.11	0.269	1.05	0.83–1.33	0.678
PCA						
RI, mean ± SD	0.96	0.89–1.04	0.283	1.00	0.93–1.08	0.911
PSV	0.96	0.88–1.04	0.289	0.99	0.91–1.08	0.832
EDV	0.93	0.75–1.16	0.517	0.94	0.75–1.18	0.603
CRV	1.01	0.90–1.15	0.827	1.02	0.90–1.15	0.765

Abbreviations: OR, Odds ratio.

*Statistically significant difference ($p < 0.05$).

pWML score (OR = 2.79, $p = 0.022$), and high RI of the OA (OR = 1.16, $p = 0.005$) in patients with minor stroke.

Multivariable logistic regression analysis was subsequently performed (Fig. 3). Variables included in the multivariable logistic regression models were selected based on both clinical relevance reported in previous studies and statistical significance in univariable analyses ($p < 0.10$). In cases where variables were highly correlated (VIF >5), only the most clinically meaningful variable was retained in the final model (**Supplementary Table 1**). As shown in Fig. 3, multivariable logistic regression analysis revealed that, after adjusting for potential covariates including age, gender, diabetes mellitus, and hypertension, SRCP perifoveal density remained significantly associated with BG-EPVS (OR = 0.87, 95% CI 0.77–0.98, $p = 0.020$), while the RI of the OA demonstrated an independent correlation with CSO-EPVS (OR = 1.33, 95% CI 1.14–1.56, $p < 0.001$). Additionally, diabetes mellitus was independently associated with BG-EPVS (OR = 2.90, 95% CI 1.08–5.80, $p = 0.035$), and the Fazekas pWML score was independently correlated with CSO-EPVS (OR = 3.38, 95% CI 1.11–5.32, $p = 0.033$). Overall, these findings indicate that, after adjusting for potential confounders, ocular vascular density is independently associated with BG-EPVS risk, whereas ophthalmic artery elasticity is independently associated with CSO-EPVS risk.

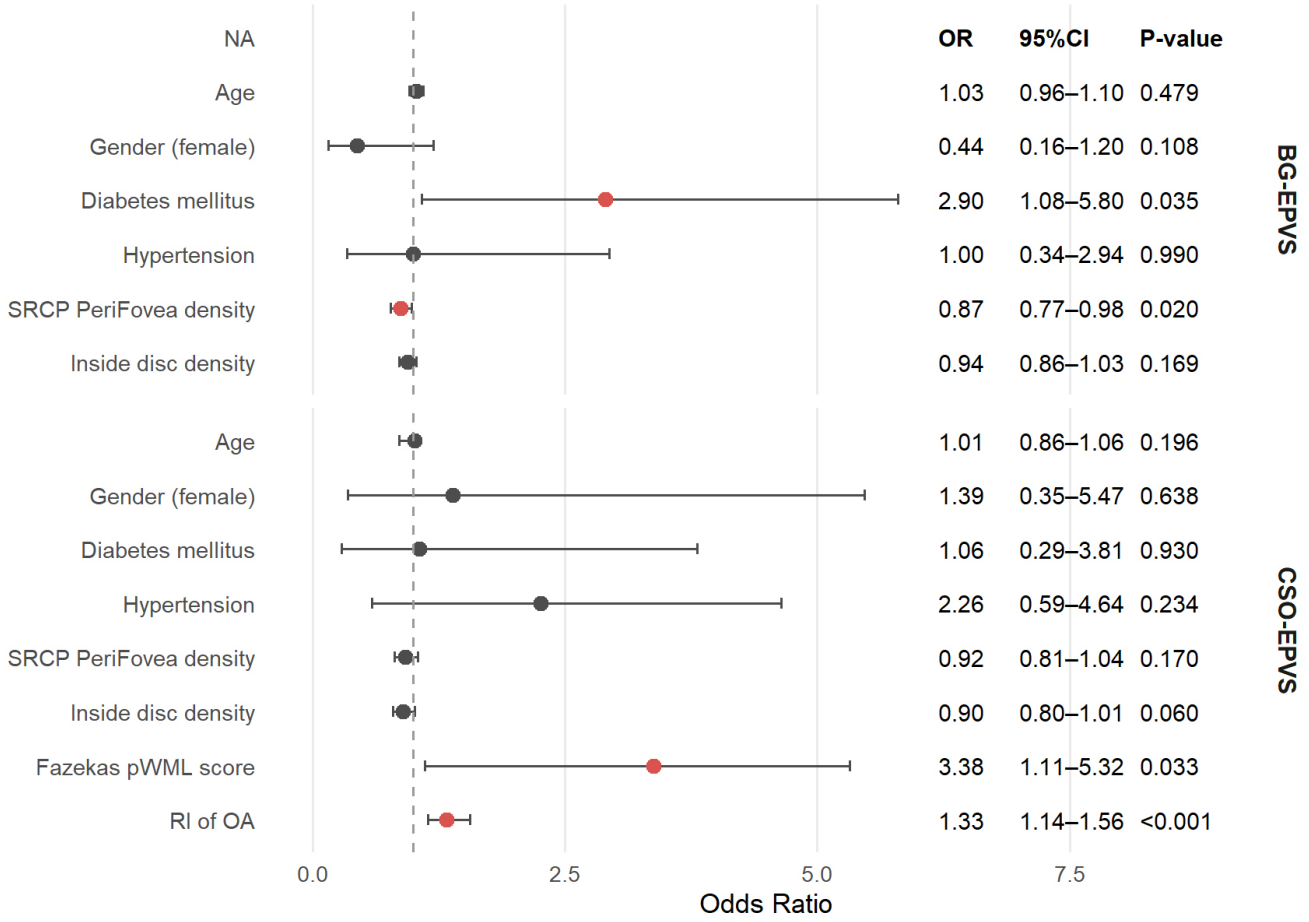

Fig. 3. Multivariate logistic regression analysis of factors associated with EPVS. A indicates variables included as risk factors in the multivariate logistic regression.

4. Discussion

In this observational study, we observed that EPVS severity and distribution varied according to ocular vascular characteristics. After adjusting for potential confounders, the perifoveal density of the superficial retinal capillary plexus measured by OCTA was independently associated with BG-EPVS, whereas the resistive index of the ophthalmic artery measured by OAU demonstrated an independent positive relationship with CSO-EPVS. These results suggest that specific microvascular and macrovascular parameters of the eye may reflect underlying cerebral small vessel pathology. By highlighting the distinct vascular correlates of BG-EPVS and CSO-EPVS, our findings contribute to a better understanding of the pathophysiological mechanisms underlying EPVS distribution and severity. This study provides novel evidence supporting the utility of noninvasive ocular vascular imaging as a potential biomarker for early identification and risk stratification of EPVS.

These findings align with prior studies reporting associations between EPVS and gender [17,18], as well as with white matter hyperintensity [19]. Moreover, we found that diabetes mellitus was positively correlated with high BG-EPVS burden, corroborating prior studies indicating that insulin resistance is positively associated with the severity of BG-EPVS [20]. Although earlier studies have reported notable links between EPVS and ocular vascular characteristics, most of these investigations were limited to a single characteristic. Mutlu *et al.* [14] reported that CRAE and central retinal vein equivalent (CRVE) were associated with the occurrence of EPVS in the CSO and hippocampus, but not in the BG. Additionally, another study observed that in patients with transient ischemic attack or minor stroke, arteriovenous nicking and retinal arteriosclerosis were positively correlated with EPVS severity [13]. Compared with these previous studies, our study provides novel insights by distinguishing region-specific associations: we demonstrate that perifoveal SRCP density is independently associated with BG-EPVS, whereas ophthalmic artery resistive index is independently associated with CSO-EPVS. This highlights the differential roles of ocular microvascular density and vascular elasticity in the pathophysiology of EPVS, offering a more nuanced understanding of eye–brain vascular interactions.

Aging, atherosclerosis, and vascular calcification progressively diminish arterial elasticity, leading to reduced ar-

terial compliance [21]. Prior research has demonstrated that markers of impaired vascular elasticity—such as decreased CRAE and increased CRVE—are associated with greater CSO-EPVS burden. A population-based cross-sectional study found that increased CRVE was associated with reduced small artery wall compliance, whereas decreased CRAE was linked to reduced large artery compliance, both of which are considered markers of endothelial dysfunction [22]. Furthermore, higher brachial–ankle pulse wave velocity (baPWV), a well-established indicator of systemic arterial stiffness, has similarly been linked to more severe CSO-EPVS [23]. These findings align with our results and support the notion that diminished vascular elasticity may impair perivascular clearance in the superficial white matter, thereby contributing to the development of CSO-EPVS. Retinal fractal dimension is commonly used to quantify retinal vascular density, and lower values indicate microvascular rarefaction. Reductions in fractal dimension (FD) have been linked to stroke, cognitive impairment, and hypertension, reflecting microvascular damage likely linked to impaired cerebral perfusion [24]. Consistent with this, our study found that lower ocular microvascular density was positively associated with higher burden of BG-EPVS, supporting the hypothesis that inadequate microcirculatory perfusion may disrupt glymphatic clearance and promote PVS enlargement in the BG. Taken together, these observations reinforce the concept that BG-EPVS and CSO-EPVS arise from distinct vascular mechanisms—microvascular hypoperfusion in deep brain regions versus reduced vascular elasticity in superficial white matter. Additionally, quantitative susceptibility mapping (QSM) reflects iron deposition and microvascular integrity. Increased susceptibility in deep gray nuclei has been linked to cognitive impairment and blood–brain barrier dysfunction in CSVD [25,26], suggesting that iron accumulation may indicate microvascular damage. Although QSM was not available in our cohort, integrating EPVS and QSM in future studies could provide complementary mechanistic insights.

The region-specific associations (BG versus CSO) could influence clinical risk stratification or follow-up strategies in patients with minor stroke or early cerebral small vessel disease. BG-EPVS may serve as an imaging marker of chronic small perforating artery injury, suggesting that patients with higher BG-EPVS burden could benefit from stricter blood pressure control and closer management of vascular risk factors. In contrast, CSO-EPVS could indicate increased upstream arterial stiffness, suggesting that patients with higher CSO-EPVS burden may benefit from systematic assessment of arterial stiffness and hemodynamic parameters, including pulse pressure and arterial resistance–related indices. Previous studies have shown that the retina and diencephalon share similar angiogenesis patterns and highly protected vascular systems, and that blood-retinal barrier dysfunction parallels blood–brain barrier impairment [27,28]. Inflammation and endothelial dysfunction, driven by common cardiovascular risk factors, may contribute to both retinal and cerebral microangiopathy [29]. Our findings suggest that ocular microvascular assessment, given its noninvasive nature, low cost, and accessibility [30], could serve as a potential biomarker for cerebral small vessel disease and may be useful for large-scale screening.

We prospectively recruited well-characterized subjects and innovatively explored the association of ocular vascular characteristics with EPVS in different regions. Simultaneously, our study represents a groundbreaking opportunity to harness noninvasive ocular microvascular measurement tools for evaluating early-stage pathological alterations in neurodegenerative diseases. Furthermore, it provides additional evidence for the different mechanisms underlying the formation of EPVS in various regions. This study had several limitations. First, although it was prospectively designed, the analysis was cross-sectional in nature. As a result, causal relationships cannot be established, and longitudinal studies are needed to determine whether ocular vascular characteristics can serve as baseline predictors of EPVS progression. Second, the cutoff of EPVS $\geq$20, while consistent with prior studies, is somewhat arbitrary, and alternative ordinal or continuous modeling approaches could provide additional insights. Moreover, despite our relatively substantial sample size, further validation of our conclusions necessitates multicenter, large-sample cohort studies. Third, EPVS were assessed visually by a senior neuroradiologist and a trained Doctor of Medicine (MD), which may introduce systematic errors. Future studies using automated or quantitative assessment with high-resolution MRI could improve measurement precision and reproducibility, potentially enhancing the robustness of the observed associations. Finally, our cohort consisted exclusively of patients with minor stroke, which may limit the generalizability of ocular–EPVS associations to community-dwelling elderly individuals or other CSVD phenotypes, such as vascular cognitive impairment. Nevertheless, as the underlying mechanisms—microvascular hypoperfusion in deep regions and reduced vascular compliance in superficial white matter—are common across CSVD, similar associations may exist in other populations. Future studies with longitudinal follow-up, multimodal imaging, mechanistic investigations, and inclusion of community-based or diverse CSVD cohorts are warranted to clarify the temporal relationship between ocular vascular alterations and EPVS progression.

5. Conclusions

In patients with minor stroke, reduced perifoveal SRCP density was associated with BG-EPVS, whereas increased ophthalmic artery resistive index was associated with CSO-EPVS, reinforcing that these EPVS subtypes arise from distinct vascular mechanisms—microvascular hypoperfusion versus reduced vascular elasticity. Noninva-

sive OCTA and OAU imaging may provide practical tools for assessing EPVS burden and early risk stratification.

Abbreviations

EPVS, enlarged perivascular spaces; OCTA, optical coherence tomography angiography; OAU, ophthalmic arterial ultrasound; MRI, magnetic resonance imaging; CSO, centrum semiovale; BG, basal ganglia; CAA, cerebral amyloid angiopathy; CSVD, cerebral small vessel disease; CT, computed tomography; NIHSS, National Institutes of Health Stroke Scale; BMI, body mass index; SRCP, superficial retinal capillary plexus; DRCP, deep retinal capillary plexus; FAZ, foveal avascular zone; VD, vessel density; ILM, internal limiting membrane; IPL, inner plexiform layer; OPL, outer plexiform layer; RNFL, retinal nerve fiber layer; OA, ophthalmic artery; CRA, central retinal artery; PCA, posterior ciliary artery; CRV, central retinal vein; PSV, peak systolic velocity; EDV, end-diastolic velocity; RI, resistive index; ICC, intraclass correlation coefficient; SD, standard deviation; IQR, interquartile range; VIF, variance inflation factor; pWML, periventricular white matter lesion; dWML, deep white matter lesion; CRAE, central retinal arteriolar equivalent; AVR, arteriole-to-venule ratio; CRVE, central retinal vein equivalent; baPWV, brachial–ankle pulse wave velocity; FD, fractal dimension; QSM, quantitative susceptibility mapping.

Availability of Data and Materials

The data that support the findings of this study are available from the corresponding authors on reasonable request.

Author Contributions

NM, JT, and QD were responsible for formal analysis and writing-review and editing; QYY, HW, PL, and QY participated in patient investigation and data curation and were responsible for writing-original draft; LG, AJ, and PG provided conceptualization and methodology. All authors contributed to editorial changes in the manuscript. All authors read and approved the final manuscript. All authors have participated sufficiently in the work and agreed to be accountable for all aspects of the work.

Ethics Approval and Consent to Participate

This study was conducted in accordance with the Declaration of Helsinki and received approval from the Ethics Committee of Shanghai Tenth People's Hospital (ethical approval number: 21K253). Written informed consent was obtained from all participants.

Acknowledgment

We thank all participants and their families, all trial investigators for their support.

Funding

This research was supported by grants from the Shanghai Municipal Science and Technology Commission (23Y11901000), National Health Commission Brain Health Innovation Research Project and National Natural Science Foundation Project (81901183).

Conflict of Interest

The authors declare no conflict of interest.

Supplementary Material

Supplementary material associated with this article can be found, in the online version, at https://doi.org/10.31083/JIN49070.

References

[1] Wardlaw JM, Smith EE, Biessels GJ, Cordonnier C, Fazekas F, Frayne R, *et al*. Neuroimaging standards for research into small vessel disease and its contribution to ageing and neurodegeneration. The Lancet. Neurology. 2013; 12: 822–838. https://doi.org/10.1016/S1474-4422(13)70124-8.

[2] Shams S, Martola J, Charidimou A, Larvie M, Granberg T, Shams M, *et al*. Topography and Determinants of Magnetic Resonance Imaging (MRI)-Visible Perivascular Spaces in a Large Memory Clinic Cohort. Journal of the American Heart Association. 2017; 6: e006279. https://doi.org/10.1161/JAHA.117.006279.

[3] Potter GM, Doubal FN, Jackson CA, Chappell FM, Sudlow CL, Dennis MS, *et al*. Enlarged perivascular spaces and cerebral small vessel disease. International Journal of Stroke: Official Journal of the International Stroke Society. 2015; 10: 376–381. https://doi.org/10.1111/ijs.12054.

[4] Bae JH, Kim JM, Park KY, Han SH. Association between arterial stiffness and the presence of cerebral small vessel disease markers. Brain and Behavior. 2021; 11: e01935. https://doi.org/10.1002/brb3.1935.

[5] Yakushiji Y, Charidimou A, Hara M, Noguchi T, Nishihara M, Eriguchi M, *et al*. Topography and associations of perivascular spaces in healthy adults: the Kashima scan study. Neurology. 2014; 83: 2116–2123. https://doi.org/10.1212/WNL.0000000000001054.

[6] Morozova A, Španiel F, Škoch A, Brabec M, Zolotarov G, Musil V, *et al*. Enlarged brain perivascular spaces correlate with blood plasma osmolality in the healthy population: A longitudinal study. NeuroImage. 2024; 300: 120871. https://doi.org/10.1016/j.neuroimage.2024.120871.

[7] Liang Y, Deng M, Chen YK, Mok V, Wang DF, Ungvari GS, *et al*. Enlarged perivascular spaces are associated with health-related quality of life in patients with acute ischemic stroke. CNS Neuroscience & Therapeutics. 2017; 23: 973–979. https://doi.org/10.1111/cns.12766.

[8] Zhuang F, Li P, He X, Shi YS, Sun LP. Risk factors for secondary enlarged perivascular spaces in patients with mild acute cerebral infarction and correlation with fundus vascular lesions. Chinese General Practice. 2023; 26: 1753–1757. https://doi.org/10.12114/j.issn.1007-9572.2022.0667. (In Chinese)

[9] Zhao B, Li Y, Fan Z, Wu Z, Shu J, Yang X, *et al*. Eye-brain connections revealed by multimodal retinal and brain imaging genetics. Nature Communications. 2024; 15: 6064. https://doi.org/10.1038/s41467-024-50309-w.

[10] Wang L, Shah S, Llaneras CN, Goldhardt R. Insight into the Brain: Application of the Retinal Microvasculature as

a Biomarker for Cerebrovascular Diseases through Optical Coherence Tomography Angiography. Current Ophthalmology Reports. 2024; 12: 1–11. https://doi.org/10.1007/s40135-023-00320-z.

[11] Wang L, Murphy O, Caldito NG, Calabresi PA, Saidha S. Emerging Applications of Optical Coherence Tomography Angiography (OCTA) in neurological research. Eye and Vision (London, England). 2018; 5: 11. https://doi.org/10.1186/s40662-018-0104-3.

[12] Wylęgała A. Principles of OCTA and Applications in Clinical Neurology. Current Neurology and Neuroscience Reports. 2018; 18: 96. https://doi.org/10.1007/s11910-018-0911-x.

[13] Huang KK, Zhang M, Pan T, Zhang ZX, Mei YQ, Li Y, *et al*. Correlation between enlarged perivascular spaces and fundus vascular lesions in patients with transient ischemic attack and minor stroke. Chinese Journal of Neurology. 2020; 53: 282–290. https://doi.org/10.3760/cma.j.cn113694-20191125-00736. (In Chinese)

[14] Mutlu U, Adams HHH, Hofman A, Lugt AVD, Klaver CCW, Vernooij MW, *et al*. Retinal Microvascular Calibers Are Associated With Enlarged Perivascular Spaces in the Brain. Stroke. 2016; 47: 1374–1376. https://doi.org/10.1161/STROKEAHA.115.012438.

[15] Zhao M, Li Y, Han X, Li C, Wang P, Wang J, *et al*. Association of enlarged perivascular spaces with cognitive function in dementia-free older adults: A population-based study. Alzheimer's & Dementia (Amsterdam, Netherlands). 2024; 16: e12618. https://doi.org/10.1002/dad2.12618.

[16] Zhu R, Li Y, Chen L, Wang Y, Cai G, Chen X, *et al*. Total Burden of Cerebral Small Vessel Disease on MRI May Predict Cognitive Impairment in Parkinson's Disease. Journal of Clinical Medicine. 2022; 11: 5381. https://doi.org/10.3390/jcm11185381.

[17] Piantino J, Boespflug EL, Schwartz DL, Luther M, Morales AM, Lin A, *et al*. Characterization of MR Imaging-Visible Perivascular Spaces in the White Matter of Healthy Adolescents at 3T. AJNR. American Journal of Neuroradiology. 2020; 41: 2139–2145. https://doi.org/10.3174/ajnr.A6789.

[18] Zhang C, Chen Q, Wang Y, Zhao X, Wang C, Liu L, *et al*. Risk factors of dilated Virchow-Robin spaces are different in various brain regions. PloS One. 2014; 9: e105505. https://doi.org/10.1371/journal.pone.0105505.

[19] Duperron MG, Tzourio C, Sargurupremraj M, Mazoyer B, Soumaré A, Schilling S, *et al*. Burden of Dilated Perivascular Spaces, an Emerging Marker of Cerebral Small Vessel Disease, Is Highly Heritable. Stroke. 2018; 49: 282–287. https://doi.org/10.1161/STROKEAHA.117.019309.

[20] Wu D, Yang X, Zhong P, Ye X, Li C, Liu X. Insulin Resistance Is Independently Associated With Enlarged Perivascular Space in the Basal Ganglia in Nondiabetic Healthy Elderly Population. American Journal of Alzheimer's Disease and other Dementias. 2020; 35: 1533317520912126. https://doi.org/10.1177/1533317520912126.

[21] Lee HY, Oh BH. Aging and arterial stiffness. Circulation Journal: Official Journal of the Japanese Circulation Society. 2010; 74: 2257–2262. https://doi.org/10.1253/circj.cj-10-0910.

[22] Cheung N, Islam FMA, Jacobs DR, Jr, Sharrett AR, Klein R, Polak JF, *et al*. Arterial compliance and retinal vascular caliber in cerebrovascular disease. Annals of Neurology. 2007; 62: 618–624. https://doi.org/10.1002/ana.21236.

[23] Brisset M, Boutouyrie P, Pico F, Zhu Y, Zureik M, Schilling S, *et al*. Large-vessel correlates of cerebral small-vessel disease. Neurology. 2013; 80: 662–669. https://doi.org/10.1212/WNL.0b013e318281ccc2.

[24] van de Kreeke JA, Nguyen HT, Konijnenberg E, Tomassen J, den Braber A, Ten Kate M, *et al*. Retinal and Cerebral Microvasculopathy: Relationships and Their Genetic Contributions. Investigative Ophthalmology & Visual Science. 2018; 59: 5025–5031. https://doi.org/10.1167/iovs.18-25341.

[25] Wang Y, Ye C, Pan R, Tang B, Li C, Liu J, *et al*. Cognitive implications and associated transcriptomic signatures of distinct regional iron depositions in cerebral small vessel disease. Alzheimer's & Dementia: the Journal of the Alzheimer's Association. 2025; 21: e70196. https://doi.org/10.1002/alz.70196.

[26] Uchida Y, Kan H, Sakurai K, Arai N, Inui S, Kobayashi S, *et al*. Iron leakage owing to blood-brain barrier disruption in small vessel disease CADASIL. Neurology. 2020; 95: e1188–e1198. https://doi.org/10.1212/WNL.0000000000010148.

[27] Cheung CYL, Ikram MK, Sabanayagam C, Wong TY. Retinal microvasculature as a model to study the manifestations of hypertension. Hypertension (Dallas, Tex.: 1979). 2012; 60: 1094–1103. https://doi.org/10.1161/HYPERTENSIONAHA.111.189142.

[28] Patton N, Aslam T, Macgillivray T, Pattie A, Deary IJ, Dhillon B. Retinal vascular image analysis as a potential screening tool for cerebrovascular disease: a rationale based on homology between cerebral and retinal microvasculatures. Journal of Anatomy. 2005; 206: 319–348. https://doi.org/10.1111/j.1469-7580.2005.00395.x.

[29] Wong SM, Jansen JFA, Zhang CE, Hoff EI, Staals J, van Oostenbrugge RJ, *et al*. Blood-brain barrier impairment and hypoperfusion are linked in cerebral small vessel disease. Neurology. 2019; 92: e1669–e1677. https://doi.org/10.1212/WNL.0000000000007263.

[30] London A, Benhar I, Schwartz M. The retina as a window to the brain-from eye research to CNS disorders. Nature Reviews. Neurology. 2013; 9: 44–53. https://doi.org/10.1038/nrneurol.2012.227.